Inverse Virtual Screening of Antitumor Targets: Pilot Study on a Small Database of Natural Bioactive Compounds

ARTICLE *in* JOURNAL OF NATURAL PRODUCTS · JUNE 2011

Impact Factor: 3.8 · DOI: 10.1021/np100935s · Source: PubMed

4 AUTHORS, INCLUDING:

Gianluigi Lauro
Università degli Studi di Salerno
17 PUBLICATIONS **116** CITATIONS
SEE PROFILE

Giuseppe Bifulco
Università degli Studi di Salerno
195 PUBLICATIONS **3,686** CITATIONS
SEE PROFILE

JOURNAL OF NATURAL PRODUCTS

ARTICLE

pubs.acs.org/jnp

Inverse Virtual Screening of Antitumor Targets: Pilot Study on a Small Database of Natural Bioactive Compounds

Gianluigi Lauro,[†] Adriana Romano,[†] Raffaele Riccio, and Giuseppe Bifulco*

Dipartimento di Scienze Farmaceutiche e Biomediche, Università di Salerno, Via Ponte Don Melillo, 84084 Fisciano (SA), Italy

Supporting Information

ABSTRACT: An inverse virtual screening in silico approach has been applied to natural bioactive molecules to screen their efficacy against proteins involved in cancer processes, with the aim of directing future experimental assays. Docking studies were performed on a panel of 126 protein targets extracted from the Protein Data Bank, to analyze their possible interactions with a small library of 43 bioactive compounds. Analysis of the molecular docking results was performed through the use of tables containing energy data organized in a matrix. The application of this approach may facilitate the prediction of the activity of unknown ligands for known targets involved in the development of cancer and could be applied to other models based on different libraries of ligands and different panels of targets.

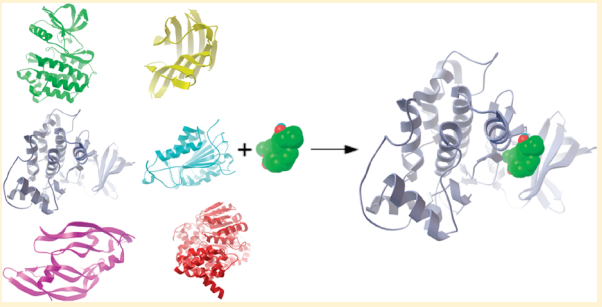

The chemistry of natural products has been investigated thoroughly in recent decades, resulting in a better understanding of enzymatic processes and in the development of biosynthetic knowledge and biogenetic theories for a logical classification connecting a large variety of compounds. Computational methods have been recently shown to be an important complementary tool for the study of the pharmacological activity of natural compounds.[1−6]

A useful approach for the study of natural products would be to carry out drug tests on a large number of biological targets with a better chance of evaluating their potential activity. However, one of the main problems in the study of natural substances is their limited availability. Unfortunately, many interesting secondary metabolites are produced by organisms in small quantities. Thus, for the isolation of a few milligrams of pure active metabolites, just enough to conduct preliminary in vitro biological tests, it is often necessary to extract kilograms of an organism. The small amounts of compounds obtained from natural sources usually prohibit the performance of pharmacological tests against a large number of receptors. One approach to possibly overcome this problem may be represented by inverse virtual screening, a new computational tool used in facilitating new drug discovery.[7−10]

We describe herein the molecular docking of a database of small natural molecules against a panel of receptor sites in an attempt to find ligands and binding conformations to direct experimental assays on specific biological targets. This approach has been applied to the discovery of potential antitumor compounds through the interaction with a number of protein targets involved in cancer. The panel of targets was built from the Protein Data Bank (PDB), by the selection of proteins involved in different forms of cancer and in several steps of tumor development and if commercially available for subsequent biological tests. The large number of available models for proteins is particularly useful for studying a wide range of molecules with variable biological activity.

It is noteworthy that this approach is also potentially applicable to libraries of synthetic compounds, to accelerate the analysis and to evaluate structure−activity relationships through a virtual method before the experimental study. The inverse virtual screening method is also useful to provide information regarding ligand−protein interactions potentially affecting the physiology of the protein. A pilot inverse virtual screening was inducted on a library of bioactive compounds ("Library on Bioactive Molecules", www.libiomol.unina.it) classified as (a) molecules with an action on the cytoskeleton; (b) cytotoxic compounds; (c) antitumor agents; (d) antiproliferative substances, and (e) antiangiogenic compounds. To the library mentioned above were added six molecules belonging to the class of cembranoids, for which the parent is decaryiol.[11,12] In total, 43 molecules were examined, comprising 27 natural compounds, three semisynthetic compounds, and 13 synthetic compounds designed for mimicking selected natural skeletons. The results obtained are reported in full in the Supporting Information, but in this paper only values concerning a small number of targets will be reported.

RESULTS AND DISCUSSION

A library of compounds was screened against a panel of targets selected for their correlations in cancer formation on the basis of the inverse virtual screening method. This innovative in silico approach allows a prediction of activity and selectivity by the evaluation of binding energies, so it is possible to obtain a restricted group of promising candidates for subsequent biological

Received: January 21, 2011
Published: May 04, 2011

Chart 1. Structures of Compounds 1−43

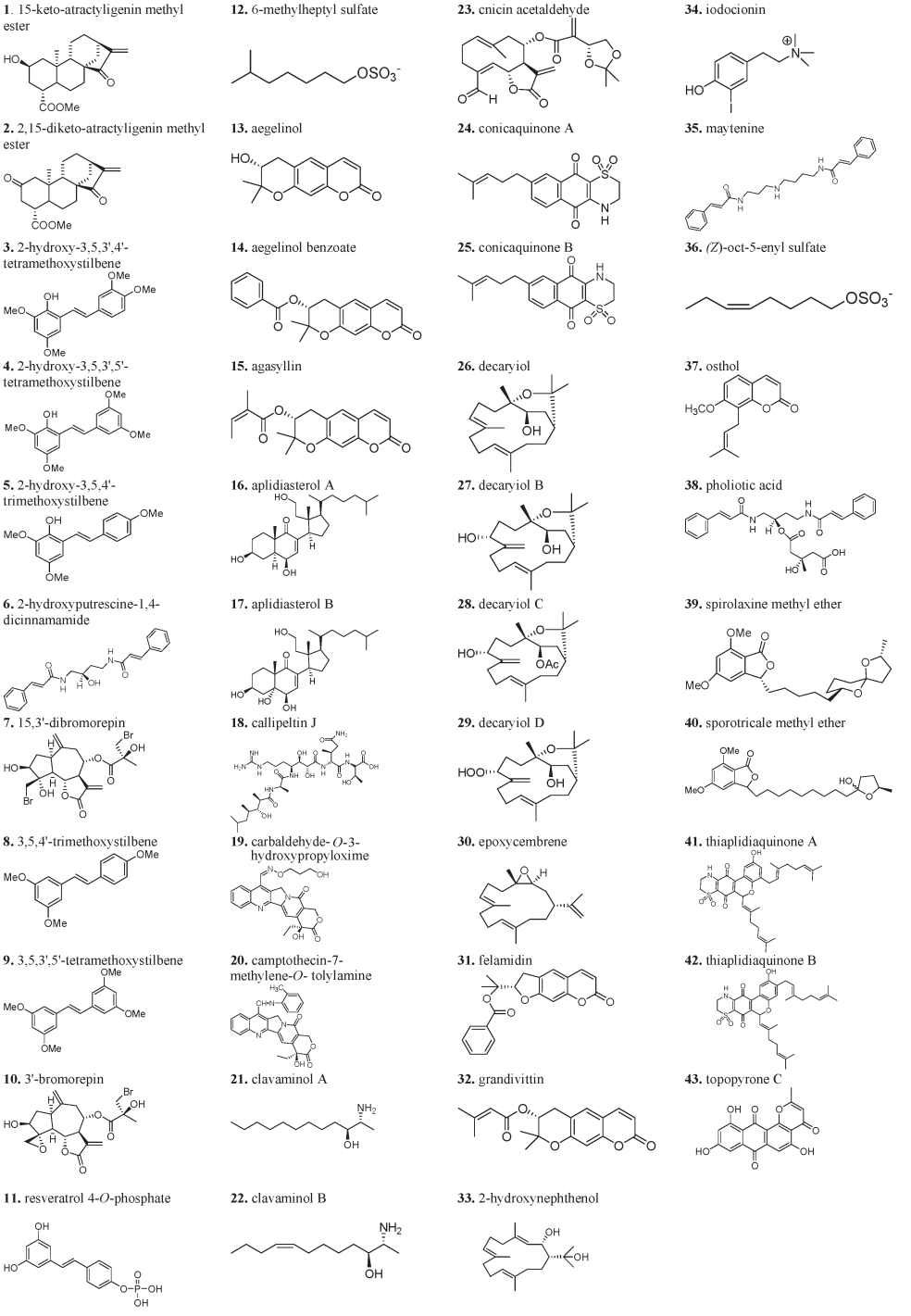

tests. In particular, Autodock−Vina[13] calculations were performed. This software has been shown to produce, together with an increased efficiency in predicting the experimental binding poses and energies, a 2 orders of magnitude speed-up compared with Autodock 4,[14] and it has been designed for parallel computing. For the above reasons, it represents a particularly suitable tool for this study, for large virtual screening studies in general, and for the investigation of ligands presenting large numbers of active torsion angles, such as naturally occurring compounds. Docking calculations were perfomed between 43 molecules (Chart 1) previously tested for their potential activity (antitumor, cytotoxic, antiangiogenic, antiproliferative, activity on the cytoskeleton) against a panel of 126 protein targets involved in tumor processes (Table S1, Supporting Information). The library used for the calculations included several types of molecules, characterized by similar or different chemical structures with known configuration.

Analysis of Predicted Binding Energies. The results of inverse virtual screening were collected in different tables and initially sorted by single ligand versus target, with the energies expressed in kcal/mol from the highest to the lowest values.

dx.doi.org/10.1021/np100935s |J. Nat. Prod. 2011, 74, 1401–1407

In this way, it was possible to identify ligands with good affinity and selectivity by evaluation of the predicted binding energies. The mere analysis of the binding energies highlighted a restricted group of targets with high values of predicted binding energies on a significant number of ligands tested (Table S2, Supporting Information), thus suggesting the use of a remodulation of the results using a different criterion.

Comparing Standard Ligands. Accordingly, docking calculations of crystallized ligands, with a well-known binding mode, were performed in order to obtain a standard energy to be introduced as a filter in the evaluation of the binding energies of the matrix used. In order to assess the efficiency of the docking experiments, the root-mean-square deviations (rmsd, expressed in Å) of the docked conformations related to the crystallized ones were calculated. Choosing a cutoff of 2 Å (an upper limit indicative of a good superimposition), 63% of the correlated structures within this range were identified (Table S3 and Figure S1, Supporting Information). This procedure was applied initially to 44 targets of the panel for which docked ligands (standards) complied with this requirement. In particular, the efficiency in the binding was evaluated through the ratio between the binding energies of the ligands and the standards, as indicated in eq 1:

$$\delta = \Delta G_{\text{compounds}}/\Delta G_{\text{standards}} \quad (1)$$

Compounds showing a $\delta \geq 1$ were selected from the library.

From this analysis, 335 associations between the ligands and the targets on 1892 calculations performed showed a $\delta \geq 1$, suggesting a consistent number of false positives (Table S4, Supporting Information). Careful analysis of the chemical structures highlighted a connection between high values of δ and high molecular weights of Libiomol ligands, especially when these were correlated to low molecular weights of standard ligands. Examples are the crystallized ligands (standards) for the targets pten (PDB code = 1D5R; standard $C_4H_6O_6$, MW = 150.09 g/mol), tp (PDB code = 1UOU; standard $C_9H_{11}ClN_4O_2$, MW = 242.66 g/mol), and clk1 (PDB code = 1Z57; standard $C_{11}H_{11}N_5O_2$, MW = 245.24 g/mol).

This trend could be explained by considering the importance of molecular size in the predicted docking energy; in particular an increase of this parameter may influence the amount of van der Waals interactions, representing an important factor for the calculations with docking software.[15]

Introducing Ligand Efficiency. For the above considerations, subsequent analysis were performed considering the "ligand efficiency" (LE) of all the molecular structures. Ligand efficiency, a term that has recently attracted the attention of researchers involved in the drug discovery field, is generally defined as the binding energy of a ligand normalized by its size.

Successful drug discovery involves the optimization of many variables, such as compound potency, selectivity, cellular activity, solubility, metabolic stability, bioavailability, and acceptable toxicity. Recently, the concept of ligand efficiency as a measure for lead selection was suggested. Ligand efficiency reduces the number of variables by combining potency with molecular weight and polar surface area. This parameter is useful for effective and efficient drug discovery and might provide the basis for a mathematically robust optimization of the drug discovery process.[16] The ligand efficiency depends on the size of the ligand, as smaller ligands have a higher efficiency than the larger ligands. One of the reasons behind this principle is the reduction in the area accessible to the ligand on increasing the size of the ligand. These findings have important implications in the screening of libraries of compounds.

Ligand efficiency is calculated using the equation

$$\text{LE} = \Delta G/N$$

where $\Delta G = RT \ln K_d$ and N is the number of non-hydrogen atoms.[16]

On this basis, we calculated the ligand efficiency of our database of compounds and for the standard ligands, and the results are reported as ratios between the values obtained for the ligands and the standards (Tables S5 and S6, Supporting Information), as indicated in eq 2:

$$\delta_{\text{LE}} = \text{LE}_{\text{compound}}/\text{LE}_{\text{standard}} \quad (2)$$

For each receptor considered, selected compounds were those complying with the following conditions:

$$\text{(a) } \delta_{\text{LE}} \geq 1; \text{ (b) } \delta_{\text{LE}} \geq M + 3\sigma$$

where M is the average value of δ_{LE} for all the compounds.

Histograms associated with each target were drawn to assess the overall behavior of the compounds analyzed for ligand efficiency. The trends observed for each target proved to be very similar, as shown in histograms reported in Figure S2 of the Supporting Information.

In a matrix of 43 compounds and 44 targets, the molecules with a low molecular weight showed the best values ($\delta_{\text{LE}} \geq 1$): 6-methylheptyl sulfate[17] and aegelinol[18−20] in docking with 18 targets; 2-hydroxynephthenol[21] in docking with eight targets; iodocionin[22] in docking with 17 targets; and (*Z*)-oct-5-enyl sulfate[17] and osthol[23,24] in docking with 17 and 14 targets, respectively. The common targets for these compounds were abl2, akt, bap1, cathepsin B, cathepsin K, cdk6, egfr, mtor, and pyk2. The most important feature of this analysis is that small molecules with a better ligand efficiency than standard ligands were selected systematically by the screening procedure.

Ligand efficiency is very important to establish limits in the building of new structures adapted on an active protein site, but the evaluation of this parameter was not considered a useful method of screening in this study.

Normalization of the Matrix. To overcome the lack of selectivity of the molecules chosen for the library to the panel of receptors, the binding energy (kcal/mol) data were organized in a matrix of 43 structures versus the 126 targets of the antitumor panel. The aim was to exclude the false positives through a mathematical filter aimed at eliminating systematic errors associated with molecules and targets in their interaction.

To obtain the normalization of binding energy values in the matrix, eq 3 was applied:

$$V = V_0/[(M_{\text{L}} + M_{\text{R}})/2] \quad (3)$$

In this convention, V is the new value associated with each compound, V_0 is the value of binding energy obtained from the docking calculation, M_{L} is the average binding energy of each ligand (on different targets), and M_{R} is the average binding energy associated with each target (on the various ligands). Every single value in the matrix representing a single ligand versus a specific receptor was accordingly normalized taking simultaneously into account the influence of the two specific averages contained in eq 3 (Table 1; the complete set of data is contained in Tables S2 and S7 of the Supporting Information).

Table 1. Values of Binding Energies for Three Sample Ligands and 33 Sample Targets

	compounds			
target	1	2	3	M_R[a]
abl	−7.5	−7.0	−7.9	−8.2
abl2	−6.2	−6.1	−8.2	−7.5
aif	−9.4	−9.3	−8.1	−8.6
akt	−8.6	−8.2	−7.1	−8.0
ape1	−6.6	−6.7	−5.7	−6.6
aurkin	−7.4	−7.0	−8.2	−8.2
bap1	−6.0	−6.0	−6.7	−7.0
bcl2	−7.9	−7.9	−6.9	−7.5
bclxl	−8.2	−8.0	−6.6	−7.4
braf	−8.6	−8.8	−7.6	−8.5
calmodulin	−6.6	−6.6	−5.7	−6.8
caspase1	−5.7	−5.5	−4.6	−5.3
caspase2	−5.2	−5.2	−4.9	−5.0
caspase3	−7.2	−7.4	−6.4	−7.1
caspase7	−8.4	−8.4	−6.8	−7.7
caspase8	−6.9	−6.9	−6.3	−6.6
cathepsin B	−8.0	−7.9	−6.4	−6.9
cathepsin G	−7.7	−7.7	−6.5	−6.8
cathepsin K	−6.3	−6.5	−5.8	−6.1
cathepsin L	−6.4	−6.1	−5.9	−6.3
cdk2	−8.5	−8.6	−7.8	−8.1
cdk6	−7.9	−8.6	−6.9	−7.8
cdk7	−8.9	−9.0	−7.8	−8.3
cdk9	−8.3	−8.4	−6.1	−7.6
chk1	−7.3	−7.4	−7.2	−7.3
chk2	−6.2	−6.3	−8.7	−8.0
ciap1	−5.9	−5.7	−5.6	−5.9
ck2	−7.8	−7.9	−7.7	−8.1
clk1	−7.6	−8.0	−7.8	−8.1
clk3	−8.7	−9.1	−7.4	−8.5
cmet	−6.4	−6.5	−7.4	−7.6
cyclin A	−7.5	−7.5	−5.5	−6.4
dhfr	−8.5	−8.5	−7.4	−7.9
M_L[b]	−7.2	−7.2	−6.6	

[a] Average of the values for targets. [b] Average of the values for ligands.

In this case, the values obtained led to the creation of histograms showing a different trend of the individual compounds against every single target, highlighting only six molecules from the entire library (Figure S3, Supporting Information). The molecules were selected through calculation of the standard deviation from the average of matrix (M); in particular the molecules were chosen up to the value of $M + 3\sigma$ to classify compounds with the best interactions. Selected results are reported in Table 2. The complete set of data is contained in Table S7 of the Supporting Information.

Analysis of the tables confirmed the validity of the method. In particular, as reported in the literature, both camptothecin-7-carbaldehyde-*O*-3-hydroxypropyloxime (**19**)[25] (Figure 1a) and camptothecin-7-methylene-*O*-tolylamine (**20**)[26] (Figure 1b) are semisynthetic derivatives of the naturally occurring camptothecin, which in biological assays show an action on topoisomerase I.[27]

Table 2. Selected Compounds after Normalization of the Matrix

compound	target	V
19	topI	1.418
20	chk2	1.446
	lsd1	1.450
	mTor	1.690
	topI	1.483
28	caspase2	1.409
31	abl2	1.398
41	mTor	1.438
43	wee1	1.429

They stimulate topoisomerase I-mediated DNA cleavage and the persistence of the cleavable complex; these compounds were evaluated for their cytotoxicity against the H460 human non-small cell lung carcinoma cell line, using topotecan as a reference compound (IC_{50} = 0.40 μM; topotecan 1.38 μM).[28] Topotecan and these compounds are very well overlapped in the pocket receptor, establishing many common interactions. From Figure 1 the accuracy of Autodock−Vina calculations on these two compounds on the panel of receptors in identifying the target of choice was clear.

The two derivatives of camptothecin establish van der Waals interactions with the same residues of the pocket occupied by topotecan (Asn722, Lys532, Asp533, Arg364), with $K_d = 2.65 \times 10^{-9}$ M (**19**) and $K_d = 2.96 \times 10^{-10}$ M (**20**). As a reference, the same Vina calculation has been performed on topotecan used as a model, and the result was −10.2 kcal/mol ($K_d = 3.34 \times 10^{-8}$ M).

Two other positive results were obtained in the calculated interactions, between the natural cytotoxic thiaplidiaquinone A[30] with the receptor mTor (PDB code = 3FAP) and the cytotoxic topopyrone C[31,32] with the receptor wee1 kinase (PDB code = 1X8B; Figure 2a).[33] Topopyrone C is very well superimposed on a crystallized inhibitor reported in the literature on wee1 kinase (9-hydroxy-4-phenylpyrrolo[3,4-*c*]carbazole-1,3(2*H*,6*H*)-dione). It establishes van der Waals interactions with Ile305, Val313, Lys323, Ala326, Phe433, and Gly382, like the crystallized ligand, with a $K_d = 1.35 \times 10^{-9}$ M, when compared with a K_d for the standard ligand of 5.81×10^{-10} M. Topopyrone C is a synthetic compound evaluated for its cytotoxicity against the H460 cell line, using topotecan as a reference compound (IC_{50} = 29.50 μM; topotecan 1.38 μM). It induces the same sequence selectivity of topoisomerase I-mediated DNA cleavage shown by camptothecin derivatives. As reported in the literature on pharmacological assays, the interaction with topoisomerase I has been found. Topotecan and topopyrone C are very well overlapped in the pocket receptor (Figure 2b); topopyrone C establishes van der Waals interactions with the same residues of the pocket occupied by topotecan (Asn722, Lys532, Asp533, and Arg364) with $K_d = 2.65 \times 10^{-9}$ M, while for topotecan the value is $K_d = 3.34 \times 10^{-8}$ M.

To obtain confirmation of the proposed method, the table organized in a matrix has been integrated with the Autodock−Vina results on two standard known molecules as ligands of the targets abl2 (PDB code = 3HMI) and FTase (PDB code = 1LD8). Both ligands (5-amino-3-{[4-(aminosulfonyl)phenyl]-amino}-*N*-(2,6-difluorophenyl)-1*H*-1,2,4-triazole-1-carbothioamide for abl2 and (20*S*)-19,20,21,22-tetrahydro-19-oxo-5*H*-18,20-ethano-12,14-etheno-6,10-metheno-18*H*-benz[*d*]imidazo[4,3-*k*][1,6,9,12]-oxatriazacyclooctadecosine-9-carbonitrile for FTase) are crystals

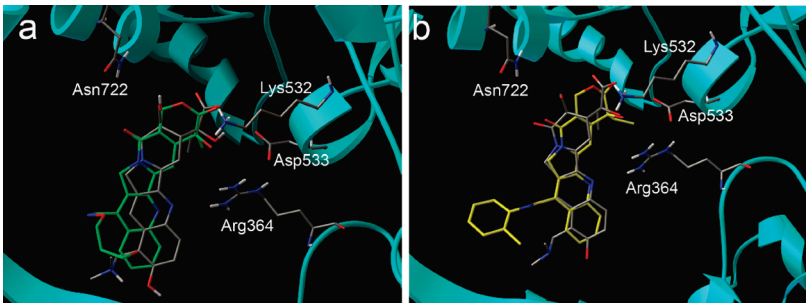

Figure 1. (a) Superimposition of topotecan (colored by atom type: O red, N blue, C gray)/camptothecin-7-carbaldehyde-*O*-3-hydroxypropyloxime (**19**) (colored by atom type: O red, N blue, C green) in docking with topoisomerase I (PDB code = 1K4T). (b) Superimposition of topotecan (colored by atom type: O red, N blue, C gray)/camptothecin-7-methylene-*O*-tolylamine (**20**) (colored by atom type: O red, N blue, C yellow) in docking with topoisomerase I.[29].

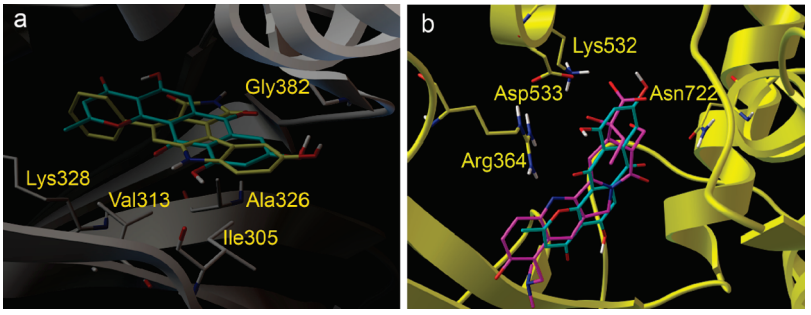

Figure 2. (a) Superimposition of 9-hydroxy-4-phenylpyrrolo[3,4-*c*]carbazole-1,3(2*H*,6*H*)-dione (colored by atom type: O red, N blue, H white, C yellow)/topopyrone C (colored by atom type: O red, N blue, H white, C cyan) in docking with wee1-kinase (PDB code = 1X8B). (b) Superimposition of topotecan (colored by atom type: O red, N blue, C pink)/topopyrone C (colored by atom type: O red, N blue, H white, C cyan) in docking with topoisomerase I (PDB code = 1K4T).

in the corresponding PDB. Docking calculations of the two compounds were performed on all the target members of the panel. The aim was to verify that the two known ligands would show significant V values when interacting with their specific target. The candidate targets for these molecules were selected through calculation of the standard deviation from the average of matrix (M) choosing V values up to $M + 3\sigma$ to classify the targets with the best interactions. For the crystallized ligand of abl2, two receptors were selected, namely, its receptor abl2 and nNos (PDB code = 3JT4). The structures obtained from Vina calculations for the abl2 ligand were very well superimposed to the crystallized compound, finding the same interactions with the receptor reported in www.pdb.org (Ligand Explorer).

On the other hand, the good interaction of the same ligand with the receptor nNos (Figure 3) is due to common interactions with its known ligand (*N*-5-[(3-(ethylsulfanyl)propanimidoyl]-L-ornithine).[34] The molecule establishes van der Waals interactions with Phe584, Glu592, and Tyr588, and one H-bond with Gln478, as reported in the literature for the crystallized ligand, and is very well accommodated in the pocket of the receptor. Also, the structure obtained from Vina calculations for FTase ligand[35] is perfectly superimposed to the crystallized compound for this receptor, displaying analogous interactions.

The data discussed above are useful to confirm the validity of the proposed computational method, and, besides the interactions with experimentally known targets, apparently discordant results are justifiable through careful analysis of the observed interactions.

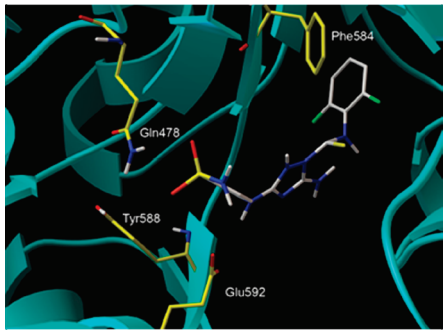

Figure 3. Interactions of the crystallized ligand of abl2 (colored by atom type: F green, O red, N blue, H and C gray) with nNos.

Classical biological assays allow the evaluation of activity associated with small molecules against one defined target protein. Thus, the main risk is to confine the study to a single effector of a pathological process. In the present report, the concept of inverse virtual screening has been introduced. The application of this method may facilitate the prediction of the activity of secondary metabolites from terrestrial and marine sources on known important receptors involved in the development of cancer. However, the variability of the binding sites of the different targets does not allow for the interpretation of docking calculations through a simple comparison of the predicted binding energies. To overcome this problem, we have applied a normalization of the matrix

that collects all values of ΔG from the calculations. In this way, some promising molecules with good superimposition with reference compounds were identified. The present results demonstrate that through Autodock−Vina calculations on large panels of ligands and targets, a screening of energies is possible in order to select the best interactions. From these selections, experimental tests could be started on a restricted number of proteins. Thus, inverse virtual screening may be considered as a new accurate tool to facilitate the drug discovery process.

EXPERIMENTAL SECTION

General Experimental Procedures. The library of compounds was downloaded from the Web site www.libiomol.unina.it. Chemical structures were processed with Macromodel 8.5 (Schrödinger, LLC, New York, 2003). Optimization (Conjugate Gradient, 0.05 Å convergence threshold) of the three-dimensional structures was applied after Monte Carlo Conformational Search and Molecular Dynamics simulations. Molecular mechanics/dynamics calculations were performed on a quad-core Intel Xeon 3.4 GHz using Macromodel 8.5 and the OPLS force field. The Monte Carlo multiple minimum (MCMM) method (5000 steps) was used first in order to allow a full exploration of the conformational space. Molecular Dynamics simulations were performed at a temperature of 600 K. A constant dielectric term, mimicking the presence of the solvent, was used in the calculations to reduce artifacts.

Protein targets, known to be involved in tumor processes, were prepared by a search of crystallized structures in the Protein Data Bank database. Water molecules were removed, and polar hydrogens were added with AutodockTools 1.4.5.

Molecular docking calculations were performed using Autodock−Vina software. The grids focused on receptors were built using as reference the binding mode of crystallized ligands in PDB files (Table S1, Supporting Information). For the docking studies, we used an exhaustiveness of 16. For all the investigated compounds, all open-chain bonds were treated as active torsional bonds. Autodock−Vina results were analyzed with Autodock Tools 1.4.5.

ASSOCIATED CONTENT

Supporting Information. PDB codes of targets with grid boxes used in calculations (Table S1), tables of data (Tables S2−S7), and graphs (Figure S1−S3) are available free of charge via the Internet at http://pubs.acs.org.

AUTHOR INFORMATION

Corresponding Author

*Tel: +39-089969741. Fax: +39-089969602. E-mail: bifulco@unisa.it.

Author Contributions

†These authors contributed equally to this work.

REFERENCES

(1) Gavernet, L.; Talevi, A.; Castro, E. A.; Bruno-Blanch, E. *QSAR Comb. Sci.* **2008**, *27*, 1120–1129.

(2) Rollinger, J. M.; Steindl, T. M.; Schuster, D.; Kirchmair, J.; Anrain, K.; Ellmerer, E. P.; Langer, T.; Stuppner, H.; Wutzler, P.; Schmidtke, M. *J. Med. Chem.* **2008**, *51*, 842–851.

(3) Schneider, G. *Nat. Rev. Drug Discovery* **2010**, *9*, 273–276.

(4) Rollinger, J. M. *Phytochem. Lett.* **2009**, *2*, 53–58.

(5) Paul, N.; Kellenberger, E.; Bret, G.; Müller, P.; Rognan, D. *Proteins: Struct., Funct. Bioinf.* **2004**, *54*, 671–680.

(6) Lamb, M. L.; Burdick, K. W.; Toba, S.; Young, M. M.; Skillman, A. G.; Zou, X.; Arnold, J. R.; Kuntz, I. D. *Proteins: Struct., Funct. Genet.* **2001**, *42*, 296–318.

(7) Chen, Y. Z.; Zhi, D. G. *Proteins: Struct., Funct. Genet.* **2001**, *43*, 217–226.

(8) Hui-Fang, L.; Qing, S.; Jian, Z.; Wei, F. *J. Mol. Graphics Modell.* **2010**, *29*, 326–330.

(9) Li, H.; Gao, Z.; Kang, L.; Zhang, H.; Yang, K.; Yu, K.; Luo, X.; Zhu, W.; Chen, K.; Shen, J.; Wang, X.; Jiang, H. *Nucleic Acids Res.* **2006**, *34*, 219–224.

(10) Zahler, S.; Tietze, S.; Totzke, F.; Kubbutat, M.; Meijer, L.; Vollmar, A. M.; Apostolakis, J. *Chem. Biol.* **2007**, *14*, 1207–1214.

(11) Carmely, S.; Groweiss, A.; Kashman, Y. *J. Org. Chem.* **1981**, *46*, 4279–4284.

(12) Fattorusso, E.; Romano, A.; Taglialatela-Scafati, O.; Irace, C.; Maffettone, C.; Bavestrello, G.; Cerrano, C. *Tetrahedron* **2009**, *65*, 2898–2904.

(13) Trott, O.; Olson, A. J. *J. Comput. Chem.* **2010**, *31*, 455–461.

(14) Huey, R.; Morris, G. M.; Olson, A. J.; Goodsell, D. S. *J. Comput. Chem.* **2007**, *28*, 1145–1152.

(15) Morris, G. M.; Goodsell, D. S.; Halliday, R. S.; Huey, R.; Hart, W. E.; Belew, R. K.; Olson, A. J. *J. Comput. Chem.* **1998**, *19*, 1639–1662.

(16) Abad-Zapatero, C.; Metz, J. T. *Drug Discovery Today* **2005**, *10*, 464–469.

(17) Aiello, A.; Carbonelli, S.; Esposito, G.; Fattorusso, E.; Iuvone, T.; Menna, M. *J. Nat. Prod.* **2000**, *63*, 517–519.

(18) Erdelmeier, C. A. J.; Sticher, O. *Planta Med.* **1985**, *51*, 407–409.

(19) Basile, A.; Sorbo, S.; Spadaro, V.; Bruno, M.; Faraone, N.; Rosselli, S. *Molecules* **2009**, *14*, 939–952.

(20) Kim, H. H.; Bang, S. S.; Choi, J. S.; Han, H.; Kim, I. H. *Cancer Lett.* **2005**, *223*, 191–201.

(21) Tursch, B.; Braekman, J. C.; Daloze, D. *Bull. Soc. Chim. Belg.* **1975**, *84*, 767–774.

(22) Aiello, A.; Fattorusso, E.; Imperatore, C.; Menna, M.; Müller, W. E. G. *Mar. Drugs* **2010**, *8*, 258–291.

(23) El-Razek, M. H. A.; Ohta, S.; Ahmed, A. A.; Hirata, T. *Phytochemistry* **2001**, *57*, 1201–1203.

(24) Rosselli, S.; Maggio, A.; Bellone, G.; Formisano, C.; Basile, A.; Cicala, C.; Alfieri, A.; Mascolo, N.; Bruno, M. *Planta Med.* **2007**, *73*, 116–120.

(25) Dallavalle, S.; Ferrari, A.; Biasotti, B.; Merlini, L.; Penco, S.; Gallo, G.; Marzi, M.; Tinti, M. O.; Martinelli, R.; Pisano, C.; Carminati, P.; Carenini, N.; Beretta, G.; Perego, P.; De Cesare, M.; Pratesi, G.; Zunino, F. *J. Med. Chem.* **2001**, *44*, 3264–3274.

(26) Dallavalle, S.; Merlini, L.; Morini, G.; Musso, L.; Penco, S.; Beretta, G.; Tinelli, S.; Zunino, F. *Eur. J. Med. Chem.* **2004**, *39*, 507–513.

(27) Burke, T. G.; Bom, D. *Ann. N.Y. Acad. Sci.* **2006**, *922*, 36–45.

(28) Kollmannsberger, C.; Mross, K.; Jakob, A.; Kanz, L.; Bokemeyer, C. *Oncology* **1999**, *56*, 1–12.

(29) Staker, B. L.; Hjerrild, K.; Feese, M. D.; Behnke, C. A.; Burgin, A. B.; Stewart, L. *Proc. Natl. Acad. Sci. U. S. A.* **2002**, *99*, 15387–15392.

(30) Aiello, A.; Fattorusso, E.; Luciano, P.; Macho, A.; Menna, M.; Muñoz, E. *J. Med. Chem.* **2005**, *48*, 3410–3416.

(31) Gattinoni, S.; Merlini, L.; Dallavalle, S. *Tetrahedron Lett.* **2007**, *48*, 1049–1051.

(32) Dallavalle, S.; Gattinoni, S.; Mazzini, S.; Scaglioni, L.; Merlini, L.; Tinelli, S.; Beretta, G. L.; Zunino, F. *Bioorg. Med. Chem. Lett.* **2008**, *18*, 1484–1489.

(33) Squire, C. J.; Dickinson, J. M.; Ivanovic, I.; Baker, E. N. *Structure* **2005**, *13*, 541–550.

(34) Martell, J. D.; Li, H.; Doukov, T.; Martásek, P.; Roman, L. J.; Soltis, M.; Poulos, T. L.; Silverman, R. B. *J. Am. Chem. Soc.* **2010**, *132*, 798–806.

(35) Bell, I. M.; Gallicchio, S. N.; Abrams, M.; Beese, L. S.; Beshore, D. C.; Bhimnathwala, H.; Bogusky, M. J.; Buser, C. A.; Culberson, J. C.;

Davide, J.; Ellis-Hutchings, M.; Fernandes, C.; Gibbs, J. B.; Graham, S. L.; Hamilton, K. A.; Hartman, G. D.; Heimbrook, D. C.; Homnick, C. F.; Huber, H. E.; Huff, J. R.; Kassahun, K.; Koblan, K. S.; Kohl, N. E.; Lobell, R. B.; Lynch, J. J., Jr.; Robinson, R.; Rodrigues, A. D.; Taylor, J. S.; Walsh, E. S.; Williams, T. M.; Zartman, C. B. *J. Med. Chem.* **2002**, *45*, 2388–2409.